Beyond Imprecise Distance Metrics: LLM-Predicted Target Call Stacks for Directed Greybox Fuzzing

YIFAN ZHANG, Peking University, China XIN ZHANG*, Peking University, China

Directed greybox fuzzing (DGF) aims to efficiently trigger bugs at specific target locations by prioritizing seeds whose execution paths are more likely to mutate into triggering target bugs. However, existing DGF approaches suffer from imprecise probability calculations due to their reliance on complex distance metrics derived from static analysis. The over-approximations inherent in static analysis cause a large number of irrelevant execution paths to be mistakenly considered to potentially mutate into triggering target bugs, significantly reducing fuzzing efficiency. We propose to replace static analysis-based distance metrics with precise call stack representations. Call stacks represent precise control flows, thereby avoiding false information in static analysis. We leverage large language models (LLMs) to predict vulnerability-triggering call stacks for guiding seed prioritization. Our approach constructs call graphs through static analysis to identify methods that can potentially reach target locations, then utilizes LLMs to predict the most likely call stack sequence that triggers the vulnerability. Seeds whose execution paths have higher overlap with the predicted call stack are prioritized for mutation. This is the first work to integrate LLMs into the core seed prioritization mechanism of DGF. We implement our approach and evaluate it against several state-of-the-art fuzzers. On a suite of real-world programs, our approach triggers vulnerabilities 1.86× to 3.09× faster compared to baselines. In addition, our approach identifies 10 new vulnerabilities and 2 incomplete fixes in the latest versions of programs used in our controlled experiments through directed patch testing, with 10 assigned CVE IDs.

1 Introduction

Directed greybox fuzzing (DGF) [2] is currently one of the most effective tools for triggering bugs at specific locations. For each seed, DGF collects its execution path and uses specific strategies to calculate the likelihood of triggering target vulnerabilities through mutation, prioritizing the mutation of seeds with higher likelihood. As a result, DGF can trigger target vulnerabilities more quickly compared to conventional coverage-guided greybox fuzzing (CGF) [32]. Research related to DGF [2, 3, 7, 10, 13–15, 18] has been widely proposed and is also extensively applied in areas such as vulnerability reproduction, patch testing, regression testing, and validation of static analysis alarms.

However, existing DGF approaches are still imprecise in calculating likelihood of triggering target vulnerabilities through mutation. Existing DGF approaches calculate likelihood based on complex distance metrics, such as distances on the control flow graph (CFG) and value flow graph (VFG). The computation of these distances is derived from over-approximations in static analysis, which inevitably leads to **many flows that do not exist during actual execution that triggers the target vulnerability**. For example, when using the state-of-the-art DGF tool DAFL [13] to trigger the known vulnerability CVE-2016-4489 [21] in cxxfilt, DAFL identified 359 critical code lines that may have potential data flow relationships with the target vulnerable statement. However, in reality, only 6 of these code lines are actually related to the target vulnerable statement. The remaining large number of irrelevant critical code lines cause DGF to spend substantial time mutating seeds whose execution paths are, in fact, difficult to mutate into target vulnerability-triggering paths, significantly reducing the efficiency of directed vulnerability triggering.

Authors' Contact Information: Yifan Zhang, Key Laboratory of High Confidence Software Technologies (Peking University), Ministry of Education; School of Computer Science, Peking University, Beijing, China, yfzhang23@stu.pku.edu.cn; Xin Zhang, Key Laboratory of High Confidence Software Technologies (Peking University), Ministry of Education; School of Computer Science, Peking University, Beijing, China, xin@pku.edu.cn.

 $^{^{*}}$ Corresponding author.

To address this issue, we propose to replace imprecise static analysis-based distance metrics and instead compute accurate call stacks as an abstract representation of the target path. Specifically, for a potential vulnerability location, we calculate the call stack sequence that triggers the vulnerability. For each seed's execution path, we use its degree of overlap with this call stack as the likelihood metric for seed prioritization. Unlike imprecise static analysis-based distance metrics, this precise call stack approach corresponds to a **sequence of precise control flows**, effectively avoiding the spurious control flows introduced by imprecise static analysis. To demonstrate the potential of this call stack-based strategy under ideal conditions, in our controlled experiments, we used the known vulnerable call stack sequence as the reference. Experimental results show that this configuration can trigger vulnerabilities 2.13× to 3.30× faster on average compared to state-of-the-art fuzzers. This demonstrates the further potential of DGF after discarding static analysis-based distance metrics. However, since the call stack that triggers the vulnerability only exists in controlled experiments, we further refine the original problem to: *How can we effectively predict the call stack that triggers a potential vulnerability*?

Given that large language models (LLMs) have demonstrated strong semantic understanding and code awareness capabilities, we propose to leverage LLMs to address this challenge. We present STACZZER, a framework that leverages LLMs to predict call stacks for guiding DGF. STACZZER first uses static analysis to construct the call graph (CG), and based on the CG, identifies all methods that might reach the potential vulnerability location through a series of calls. STACZZER then incorporates the source code of these methods into the prompt provided to the LLM, enabling the prediction of a call stack that is then used to guide seed prioritization in DGF. Experimental results show that the call stacks predicted by the LLM can achieve a high level of accuracy, and the acceleration effect on DGF closely approximates the configuration that uses known call stacks. Additionally, unlike previous work [37] that merely employs LLMs to assist DGF in generating initial seeds more prone to triggering vulnerabilities, our work is the first to integrate LLMs into the core seed prioritization module of DGF. As LLM capabilities continue to advance, DGF is expected to benefit from increasingly accurate call stack predictions for more complex programs.

We have implemented STACZZER on top of the DGF framework DAFL [13], and compared it against the following state-of-the-art fuzzers: (1) AFLGO [2], the first DGF tool, which employs complex distance metrics based on CFG; (2) WINDRANGER [7], an optimized DGF that builds upon AFLGO by computing only deviation basic blocks (DBBs); (3) DAFL [13], which utilizes complex distance metrics based on VFG; (4) AFL [32], the base framework for all fuzzers used in our evaluation. We use the same set of 41 real-world known vulnerabilities and evaluation metrics as DAFL. The results show that STACZZER triggers vulnerabilities on average 3.09×, 2.43×, 1.86×, and 2.03× faster than these baselines. Furthermore, by performing directed testing on existing patch locations in the latest versions of controlled experiment benchmarks, STACZZER successfully discovered 10 new vulnerabilities and 2 incomplete fixes in high-impact software GNU linker and its related Binutils components, with 10 assigned CVE IDs.

Contributions. This paper makes the following contributions:

- (1) We address the imprecise conventional distance metrics in DGF by introducing precise call stacks to better measure the likelihood of triggering target vulnerabilities through mutation.
- (2) We present STACZZER, a framework that integrates LLM-based prediction of vulnerability-triggering call stacks to guide DGF.
- (3) We are the first to integrate LLMs into the core seed prioritization module of DGF, which more effectively utilizes LLM capabilities for enhancing DGF performance.
- (4) We show the effectiveness of STACZZER on a suite of real-world programs. STACZZER demonstrates significantly stronger vulnerability triggering performance compared to the baselines.

```
20
                                                                      (*output) += 12:
1
    char** output:
                                                                      gnu_special(mangled);
                                                            21
2
    void gnu_special(const char** mangled){
                                                            22
                                                                    }
4
     if('0' <= **mangled && **mangled <= '9'){</pre>
                                                           23
                                                                  }else{
        int n = 0;
                                                                    if(strlen(*mangled) >= 9 && strncmp(*mangled, "
5
                                                           24
        while('0' <= **mangled && **mangled <= '9'){</pre>
                                                                          _GLOBAL_", 8) == 0 && !('0' <= (*mangled)
6
                                                                          [8] && (*mangled)[8] <= '9')){
7
8
          n += **mangled - '0';
                                                            25
                                                                      (*mangled) += 8;
         (*mangled)++;
9
                                                           26
                                                                      gnu_special(mangled);
10
                                                            27
        memcpy(*output, *mangled, n); // CVE-2016-4489
                                                            28
                                                                  }
11
12
      }
                                                            29
13
                                                            30
                                                                }
    }
                                                            31
14
15
                                                            32
                                                                  const char** mangled = input1();
16
    void internal_cplus_demangle(const char** mangled,
                                                            33
          bool flag){
                                                                  bool flag = input2();
                                                           34
17
      if(flag){
                                                           35
                                                                 internal_cplus_demangle(mangled, flag);
        if(**mangled != '\0'){
                                                           36
          memcpy(*output, "cplus_marker", 12);
                                                           37 }
19
```

Fig. 1. Simplified code fragment from cxxfilt containing CVE-2016-4489.

2 Motivating Example

In this section, we demonstrate the limitations of existing DGF approaches that use imprecise distance metrics to determine which seeds are more likely to mutate into inputs that trigger target vulnerabilities. We use the triggering of CVE-2016-4489 [21] in cxxfilt as a case study to illustrate these limitations, and subsequently show how our approach effectively addresses this problem.

2.1 A Seed Prioritization Problem in Directed Greybox Fuzzing

Figure 1 presents the simplified code containing CVE-2016-4489 in cxxfilt. For brevity, we have modified the code while preserving the semantics relevant to the vulnerability. cxxfilt demangles C++ symbols by reversing the name mangling performed by compilers on function names, class names, and other symbols, restoring them to human-readable form. Starting from Line 33, the code reads the mangled input from the input1 function and passes its address to the variable mangled. Subsequently, at Line 34, the code reads a boolean value from the input2 function as the value for variable flag, which will determine the control flow in subsequent functions. Next, at Line 35, the code calls the function internal_cplus_demangle with the aforementioned two parameters to begin the demangling operation. In this function, the code first checks the value of flag at Line 17 to determine which branch to follow. We explain these two branches sequentially:

- (1) When flag is true, the code first checks at Line 18 whether the mangled string mangled is empty. If not, it continues with parsing. The pointer output defined at Line 1 points to allocated memory representing the parsing information for output. The code writes information to the output buffer at Line 19, then advances the output buffer pointer at Line 20, and finally performs further demangling of special symbols at Line 21 by invoking the function gnu_special.
- (2) When flag is false, the code checks at Line 24 whether the mangled string mangled starts with _GLOBAL_ and the next character is not a digit. If so, it completes parsing of _GLOBAL_

Seed	input1	input2
s ₀	Alice	true
	CLODAL Dob	£-1

Table 1. Information of two seeds s_0 and s_1 .

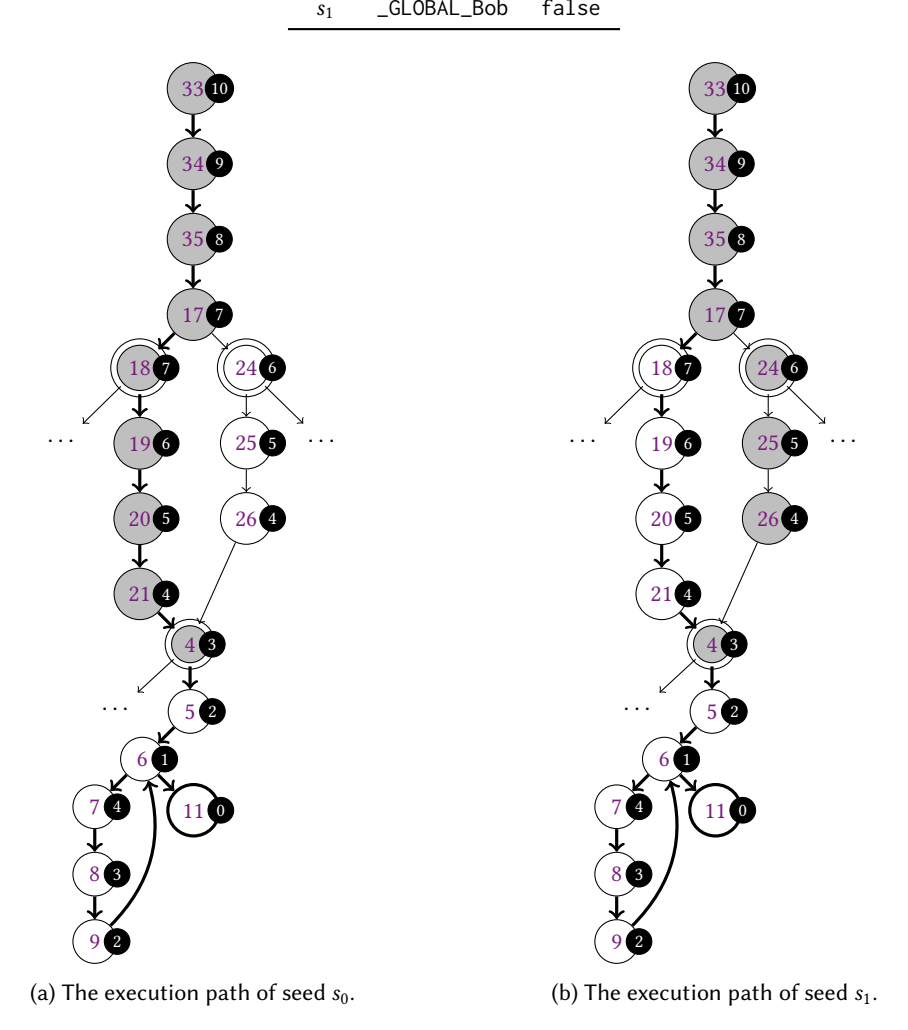


Fig. 2. CFG corresponding to the code fragment in Figure 1 and the nodes traversed by the execution paths of seeds s_0 and s_1 . The numbers within each node represent the line numbers in Figure 1, while the numbers in the small circles to the right of each node indicate their shortest distances to the target node. Nodes with gray backgrounds represent the nodes traversed by the seed's execution path. Nodes with double borders represent deviation basic blocks (DBBs) as defined in Windranger, which can reach the target node themselves but point to a node that cannot reach the target node. Nodes with bold borders represent target nodes. Bold edges represent the control flows present in the actual vulnerability-triggering execution.

and advances the mangled pointer at Line 25, then performs further demangling of special symbols at Line 26 by invoking the function gnu_special.

In the gnu_special function, the code first checks at Line 4 whether the mangled string mangled starts with a digit. If so, from Line 5 to Line 9, it reads a complete string until the next character is not a digit, storing this integer as the value of variable n. Finally, the code reads n characters from the mangled string mangled into the output buffer at Line 11. However, since no range validation is performed when computing n, if it becomes a very large value or overflows to a negative value, a segmentation fault will occur at Line 11. This is the root cause of CVE-2016-4489.

Currently, DGF has two seeds s_0 and s_1 , and DGF needs to determine which seed is more worthy of priority mutation. The information of the two seeds is shown in Table 1. Both s_0 and s_1 have input1 that does not contain any digits, so neither can directly trigger the target vulnerability. However, s_0 has input2 set to true while s_1 has it set to false. If input2 remains false, it is impossible to trigger the target vulnerability because when flag is false, the code will execute the second branch of internal_cplus_demangle. In this case, the condition in Line 24 checks that the first character processed in Line 4 is not a digit, making it impossible to execute the code at Line 11 under any circumstances. In summary, s_0 is more worthy of priority mutation compared to s_1 , as it only needs to mutate the beginning of input1 to a large number to trigger the vulnerability, while s_1 would additionally need to mutate input2 to true. We will demonstrate the limitations of existing approaches that employ imprecise distance metrics for this seed prioritization problem in the next subsection.

2.2 Limitations of Existing Approaches with Imprecise Score Metrics

We demonstrate the limitations of three state-of-the-art DGF approaches that use imprecise distance metrics when addressing the aforementioned problem: AFLGo [2], WindRanger [7], and DAFL [13]. They guide DGF seed prioritization through imprecise results derived from static analysis, causing control flows or data flows that do not exist in actual vulnerability-triggering executions to incorrectly select seeds that are more likely to mutate into vulnerability-triggering inputs.

We first demonstrate how AFLGo [2] addresses this problem. For each seed's execution path, AFLGo calculates the control flow graph (CFG) nodes it traverses and computes the harmonic mean of their shortest distances to the target statement node, as shown in Figure 2. AFLGo considers seeds with shorter average distances to be easier to mutate into vulnerability-triggering inputs, and therefore prioritizes their mutation. According to this calculation method, the scores for selecting between s_0 and s_1 are computed as follows:

$$SCORE_{AFLGo}(s_0) = \underbrace{\left(\underbrace{\begin{array}{c} Node \ 33 \quad Node \ 34 \quad Node \ 34 \quad Node \ 35 \quad Node \ 17 \quad Node \ 18 \quad Node \ 19 \quad Node \ 20 \quad Node \ 21 \quad Node \ 4}_{9^{-1} \quad + \quad 9^{-1} \quad + \quad 9^{-1} \quad + \quad 9^{-1} \quad + \quad 10^{-1} \quad + \quad 10^{-1$$

Since $Score_{AFLGo}(s_0) > Score_{AFLGo}(s_1)$, AFLGo would prioritize mutating s_1 , which is an incorrect and inefficient choice. AFLGo fails to correctly select s_0 because the CFG contains control flows that do not exist in vulnerability-triggering executions (i.e., those edges that are not bolded in Figure 2).

These edges cause nodes 24, 25, and 26, which originally do not have vulnerability-triggering control flows, to be assigned shorter distances than nodes 18, 19, and 20 due to the imprecise results of static analysis.

We next demonstrate how Windranger [7] addresses this problem. Windranger introduces the concept of deviation basic blocks (DBBs). DBBs are nodes in the control flow graph that can reach the target node themselves but point to nodes that cannot reach the target node. DBBs are represented with double borders in Figure 2. Windranger argues that AFLGo's approach of including the distances of all nodes to the target in the calculation causes the average distance to be diluted by numerous irrelevant nodes. Therefore, Windranger only considers the distances from DBBs to the target node, prioritizing seeds with smaller arithmetic averages for mutation. According to this calculation method, the scores for selecting between s_0 and s_1 are computed as follows:

$$SCORE_{WINDRANGER}(s_0) = \frac{\overbrace{7 + 3}^{Node 18} - Node 4}{2} = 5$$

$$SCORE_{WINDRANGER}(s_1) = \frac{\overbrace{6 + 3}^{Node 24} - Node 4}{2} = 4.5$$

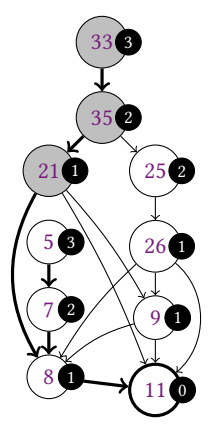
Since $Score_{WindRanger}(s_0) > Score_{WindRanger}(s_1)$, WindRanger would prioritize mutating s_1 , which is still an incorrect and inefficient choice. WindRanger makes the same incorrect choice as AFLGo. This is because although WindRanger does avoid dilution from unimportant nodes, it still cannot avoid the impact of imprecise control flows. DBB 24 does not have control flows reaching the target in vulnerability-triggering executions, yet it is calculated to have a smaller distance than DBB 18, ultimately leading to WindRanger's incorrect decision.

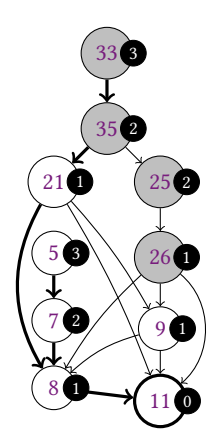
Finally, we demonstrate how DAFL [13] addresses this problem. DAFL argues that the control flows described by CFG cannot provide sufficiently precise feedback for fuzzers. Therefore, it adopts the more accurate value flow graph (VFG). Only edges with potential data flow appear in the VFG, avoiding numerous useless edges compared to CFG. For each seed's execution path, DAFL calculates the VFG nodes it traverses, as shown in Figure 3. DAFL performs seed prioritization based on their shortest distances to the target statement node. The specific calculation method assumes that the farthest distance from all nodes to the target node is L (L = 3 in our example). For a node at distance i from the target node, its score is L - i + 1. DAFL considers seeds that traverse nodes with higher total scores to be easier to mutate into vulnerability-triggering inputs. According to this calculation method, the scores for selecting between s_0 and s_1 are computed as follows:

$$SCORe_{DAFL}(s_0) = \overbrace{L - 3 + 1 + L - 2 + 1}^{Node 33} + \overbrace{L - 1 + 1}^{Node 35} = 6$$

$$SCORe_{DAFL}(s_1) = \overbrace{L - 3 + 1 + L - 2 + 1}^{Node 33} + \overbrace{L - 2 + 1 + L - 2 + 1}^{Node 25} + \overbrace{L - 1 + 1}^{Node 26} = 8$$

Since $Score_{DAFL}(s_0) < Score_{DAFL}(s_1)$, DAFL would prioritize mutating s_1 . DAFL makes the same incorrect choice as AFLGo and Windranger. This is because although VFG does filter out many meaningless control flows in CFG, VFG itself is still an imprecise result derived from static analysis. Therefore, it still contains data flows that do not exist in actual vulnerability-triggering executions. Nodes 25 and 26 are incorrectly calculated to have vulnerability-triggering data flows. This imprecise result causes DAFL to compute a higher score for s_1 .





- (a) The execution path of seed s_0 .
- (b) The execution path of seed s_1 .

Fig. 3. VFG corresponding to the code fragment in Figure 1 and the nodes traversed by the execution paths of seeds s_0 and s_1 . The numbers within each node represent the line numbers in Figure 1, while the numbers in the small circles to the right of each node indicate their shortest distances to the target node. Nodes with gray backgrounds represent the nodes traversed by the seed's execution path. Nodes with bold borders represent target nodes. Bold edges represent the value flows present in the actual vulnerability-triggering execution.

In summary, we have demonstrated the limitations of three state-of-the-art DGF approaches that use imprecise distance metrics. Although they are based on different measurement methods (CFG, DBB, VFG), they all directly use the results of static analysis. However, static analysis results can never achieve complete accuracy [25]. Therefore, these DGF approaches inevitably suffer from misleading imprecise analysis results during seed prioritization. In practice, DGF performs separate compilation for each version of each software. The excessive time required for static analysis would severely impact DGF efficiency. Consequently, various DGF tools employ lightweight but coarse-grained static analysis. This leads to numerous imprecise analysis results, severely exacerbating this problem. To address this issue, we need to find more precise information beyond static analysis to guide DGF in seed prioritization.

2.3 Our Approach

We propose STACZZER, a novel DGF framework that abandons imprecise distance metrics from static analysis. Instead, STACZZER uses call stacks predicted by large language models (LLMs) as more precise information to guide DGF seed prioritization. Our intuition for choosing call stacks as the abstract representation of target paths, rather than more precise information (such as basic block-level precise control flows), is twofold:

- (1) Call stacks are sufficiently coarse-grained while capturing control flow information, enabling existing LLMs to predict them effectively. More complex information would be difficult for LLMs to predict accurately.
- (2) Call stack traces when vulnerabilities occur are common in actual software engineering. For example, Figure 4 shows the call stack trace generated by AddressSanitizer [27] after triggering vulnerability CVE-2017-8398 [22]. Compared to more complex information, LLMs have a deeper understanding of such widely-recognized concepts, enabling them to provide more accurate predictions.

```
1
         x7ffda177cbd0 sp 0x7ffda177c350
 2
    READ of size 1 at 0x60800000007d thread T0
3
       #0 0x43a8f0 in printf_common(void*, char const*, __va_list_tag*) /src/llvm-project/compiler-rt/lib/
             sanitizer_common/sanitizer_common_interceptors_format.inc:553:9
       #1 0x43bcca in __interceptor_vprintf /src/llvm-project/compiler-rt/lib/sanitizer_common/
             sanitizer_common_interceptors.inc:1643:1
 5
       #2 0x43bcca in printf /src/llvm-project/compiler-rt/lib/sanitizer_common/sanitizer_common_interceptors.
             inc:1701:1
       #3 0x5058d5 in process_extended_line_op /benchmark/binutils/dwarf.c:484:7
6
       #4 0x5058d5 in display_debug_lines_raw /benchmark/binutils/dwarf.c:3045:18
       #5 0x4e99de in display_debug_lines /benchmark/binutils/dwarf.c:3737:17
8
       #6 0x4cf00a in dump_dwarf_section /benchmark/binutils/objdump.c:2555:6
10
       #7 0x5f964b in bfd_map_over_sections bfd/section.c:1395:5
       #8 0x4ce237 in dump_dwarf /benchmark/binutils/objdump.c:2621:3
11
12
       \#9 0x4cb35b in dump_bfd /benchmark/binutils/objdump.c:3459:5
       #10 0x4ca225 in display_object_bfd /benchmark/binutils/objdump.c
13
       #11 0x4ca225 in display_any_bfd /benchmark/binutils/objdump.c:3615:5
14
15
       #12 0x4c98ec in display_file /benchmark/binutils/objdump.c:3636:3
       #13 0x4c98ec in main /benchmark/binutils/objdump.c:3919:4
16
```

Fig. 4. Call stack backtrace generated by AddressSanitizer after triggering vulnerability CVE-2017-8398.

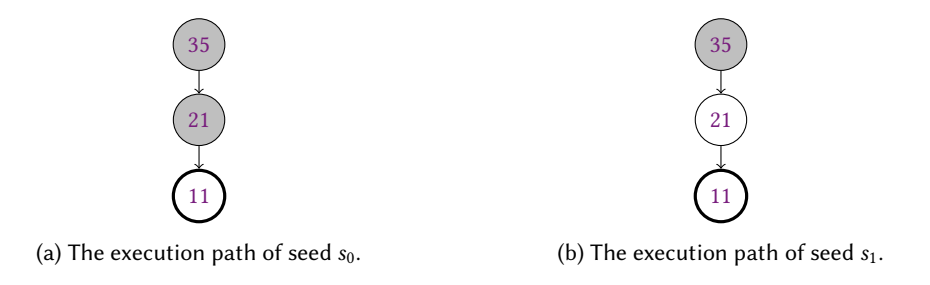


Fig. 5. Call stack corresponding to the code fragment when triggering the target vulnerability in Figure 1 and the nodes traversed by the execution paths of seeds s_0 and s_1 . The numbers within each node represent the line numbers in Figure 1. Nodes with gray backgrounds represent the nodes traversed by the seed's execution path. Nodes with bold borders represent the target code line. Nodes without bold borders represent call sites in vulnerability-triggering execution.

Next, we demonstrate how STACZZER addresses the seed prioritization problem in our case study. We will provide a detailed description of STACZZER's interaction with LLMs in Section 4. Here, we assume that the LLM has successfully generated the call stack for triggering the vulnerability:

Line
$$35 \rightarrow \text{Line } 21 \rightarrow \text{Line } 11$$

STACZZER uses consecutive call sites from the outermost entrance function to the function containing the target statement, along with the final target statement, as the call stack for vulnerability-triggering execution. For each seed's execution path, STACZZER calculates how many statements in the call stack it traverses, as shown in Figure 5. STACZZER considers seeds that traverse more statements to have a higher probability of mutating into vulnerability-triggering inputs. According

to this calculation method, the scores for selecting between s_0 and s_1 are computed as follows:

$$SCORE_{STACZZER}(s_0) = \overbrace{1}^{Node 35} + \overbrace{1}^{Node 21} = 2$$

$$SCORE_{STACZZER}(s_1) = \overbrace{1}^{Node 35} = 1$$

Since $Score_{Staczzer}(s_0) > Score_{Staczzer}(s_1)$, Staczzer would prioritize mutating s_0 . Staczzer successfully makes the correct choice, owing to its use of precise call stack information to guide DGF, effectively avoiding all misleading imprecise analysis results. The call stack clearly indicates that the call site Line 21 is a necessary path for triggering the vulnerability. Therefore, Staczzer prioritizes seed s_0 that satisfies this condition, rather than s_1 which deviates from this call site. Next, we provide the formal preliminaries in Section 3, and present the detailed workflow of the Staczzer framework in Section 4.

3 Preliminaries

For the program to be fuzzed, we provide the following formal definitions for the relevant content.

Definition 3.1 (program input). We define S as the set of program inputs. Each s ∈ S represents a possible input to the program.

Example 3.2. In the example shown in Section 2, we have $s_0, s_1 \in S$.

Definition 3.3 (program location). We define L as the set of program locations. Each $l \in L$ represents a specific line of code in the program.

Example 3.4. In the example shown in Section 2, we have Line 33, Line 20, Line $11 \in L$.

Definition 3.5 (crashing input). A crashing input $s \in S$ refers to an input that causes the program to crash at program location $l \in L$ when executed with this input. We use a function Crashing $(S, l) : S \times L \to \{\text{true}, \text{false}\}$ to represent whether input s causes the program to crash at location l.

Example 3.6. In the example shown in Section 2, we have Crashing(s_0 , Line 11) = false and Crashing(s_1 , Line 11) = false. Consider the following input s_2 :

We have $Crashing(s_2, Line 11) = true$.

Definition 3.7 (execution trace). The execution trace of an input $s \in S$ refers to all program locations traversed when the program runs with this input. We use a function Trace(s) : $S \to \mathcal{P}(L)$ to represent the set.

Example 3.8. In the example shown in Section 2, we have:

```
Trace(s_0) ={Line 33, Line 34, Line 35, Line 17, Line 18, Line 19, Line 20, Line 21, Line 4}
Trace(s_1) ={Line 33, Line 34, Line 35, Line 17, Line 24, Line 25, Line 26, Line 4}
```

Definition 3.9 (goal of directed greybox fuzzing). The goal of directed greybox fuzzing is to generate an input $s \in S$ such that Crashing(s, l_{target}) = true for a given target location $l_{\text{target}} \in L$ in the shortest possible time.

Definition 3.10 (call graph). We define F as the set of all functions in the code. We define the call graph as a directed graph (V, E), where V = F, and each edge $(i, j, l) \in E$ indicates that function $i \in F$ may have a call site $l \in L$ that invokes function $j \in F$.

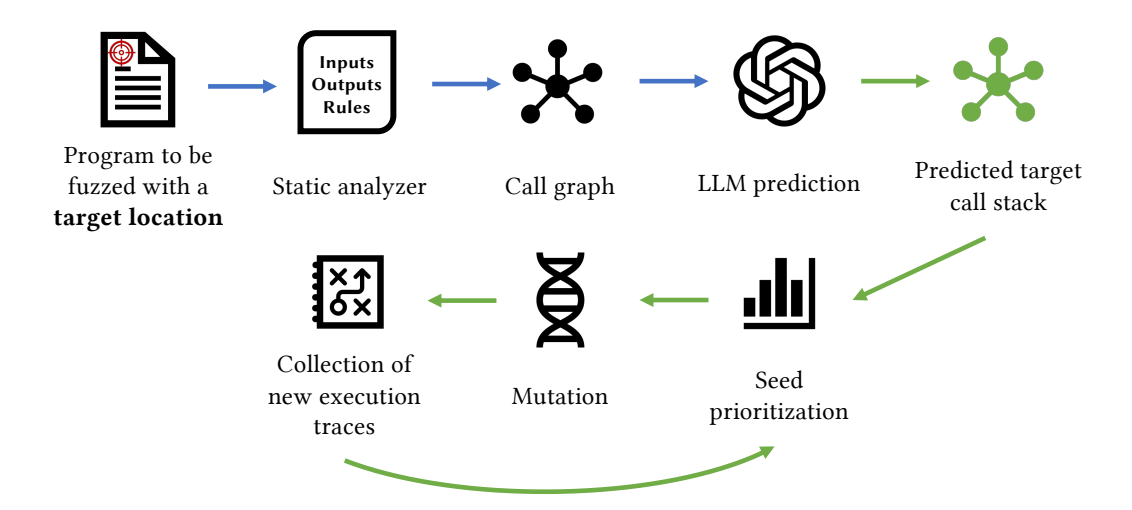


Fig. 6. Overview of framework Staczzer that leverages LLM-predicted target call stacks to guide directed greybox fuzzing.

Example 3.11. In the example shown in Section 2, a possible call graph is as follows:

```
V = \{ \texttt{gnu\_special}, \texttt{internal\_cplus\_demangle}, \texttt{main} \} E = \left\{ \begin{aligned} &(\texttt{main}, \texttt{internal\_cplus\_demangle}, \texttt{Line 35}), \\ &(\texttt{internal\_cplus\_demangle}, \texttt{gnu\_special}, \texttt{Line 21}), \\ &(\texttt{internal\_cplus\_demangle}, \texttt{gnu\_special}, \texttt{Line 26}) \end{aligned} \right.
```

4 The STACZZER Framework

Figure 6 shows the workflow of the STACZZER framework. Given a program under test and a target location that may contain potential vulnerabilities, STACZZER uses static analysis to construct a call graph. For all functions that may reach the function containing the target location through several calls, STACZZER integrates their source code and submits it to the LLM using a specific prompt template. The LLM then provides a prediction of the target call stack. STACZZER leverages the overlap between each seed and this call stack to perform seed prioritization. STACZZER then mutates the selected seed, collects new execution traces, and repeats the process for the next round of seed prioritization. We formalize the algorithmic workflow of STACZZER in Section 4.1, followed by formal descriptions of LLM prediction of target call stack and seed prioritization in Section 4.2 and Section 4.3, respectively.

4.1 Overview

Algorithm 1 formalizes the workflow of Staczzer. The workflow of Staczzer is based on directed greybox fuzzing (DGF), with all lines that differ from DGF highlighted in gray shade. Staczzer takes as input an initial seed set $S_0 \subseteq S$ and a target program location $l_{\text{target}} \in L$. Staczzer outputs the set of all inputs that can trigger program crashes S_{\times} . Staczzer maintains the current seed set S (initially S_0) and the current crashing seed set S_{\times} (initially empty) (Line 2), then uses LLM to predict the call stack $L_{\text{predicted}} \subseteq L$ for triggering vulnerabilities at target l_{target} (Line 3, detailed in Section 4.2). Staczzer then continuously repeats the following fuzzing process (Line 4):

Algorithm 1 The STACZZER framework.

```
Input: The set of initial seeds S_0, and the target program location l_{\text{target}}.
Output: The crashing seeds set S_{\times}.
  1: procedure Staczzer(S_0, l_{\text{target}})
            S \leftarrow S_0, S_{\times} \leftarrow \emptyset
  2:
             L_{\text{predicted}} \leftarrow \text{PredictCallStack}(l_{\text{target}})
  3:
            repeat
  4:
                   s \leftarrow \text{ChooseSeed}(S, L_{\text{predicted}})
  5:
                   e \leftarrow AssignEnergy(S, s, L_{predicted})
  6:
  7:
                  \mathbf{for}\ i = 1 \to e\ \mathbf{do}
  8:
                       s' \leftarrow \text{MUTATE}(s)
                       if Trace(s') \notin {Trace(s) | s \in S} then
  9:
                             S \leftarrow S \cup \{s'\}
10:
                             if \exists l \in L such that Crashing(s, l) = \text{true then}
11:
                                   S_{\times} \leftarrow S_{\times} \cup \{s'\}
12:
            until timeout
13:
14:
            return S_{\times}
```

- (1) STACZZER selects the seed s ∈ S to prioritize for mutation in the current round based on call stack L_{predicted} (Line 5, detailed in Section 4.3), then assigns energy e ∈ N based on call stack L_{predicted} to represent the number of mutations for this round (Line 6, detailed in Section 4.3). Higher energy indicates greater importance and requires more time allocation for mutation.
- (2) Based on the assigned energy *e*, STACZZER mutates seed *s* for *e* times (Line 7), with each mutation calling MUTATE(*s*) to generate a new seed *s'* (Line 8). MUTATE(*s*) follows the same settings as AFL [32], randomly selecting a mutator (such as randomly flipping a bit, randomly adding/subtracting values to a byte, deleting random-length bytes, etc.) to modify *s*.
- (3) For the new seed s', if its execution trace differs from all existing seeds (Line 9), this new seed will be retained (Line 10). Additionally, if this seed causes a crash (Line 11), it will also be saved in S_{\times} (Line 12).

Finally, when time runs out (Line 13), STACZZER returns the set of all crashing seeds S_{\times} (Line 14). The design goal of STACZZER is to generate an s' (Line 8) such that CRASHING(s', l_{target}) = true as quickly as possible.

4.2 LLM Prediction of Target Call Stack

Algorithm 2 formalizes the algorithm to leverage LLM to predict target call stack in the Staczzer framework. The algorithm takes as input a target program location $l_{\text{target}} \in \mathbf{L}$ and outputs the call stack $L_{\text{predicted}} \subseteq \mathbf{L}$ predicted by LLM for triggering potential vulnerabilities at l_{target} . Staczzer first obtains a call graph (V, E) based on static analysis (Line 2). Then, for the function f_{target} containing l_{target} (Line 3), Staczzer finds all functions $F_{\text{reachable}}$ that can reach f_{target} in the call graph (Line 4). For each function f in $F_{\text{reachable}}$, Staczzer concatenates their source code together to obtain $C_{\text{reachable}}$ (Line 5). To help LLM better understand and locate information in the code, we make two improvements to $C_{\text{reachable}}$:

- (1) We mark the file name and function name at the beginning of each function.
- (2) We add comments indicating the file and line number for all call sites that may reach l_{target} and the target line l_{target} itself.

Algorithm 2 The algorithm to predict target call stack in the STACZZER framework.

Input: The target program location l_{target} .

Output: The set of program locations in the predicted target call stack $L_{\text{predicted}}$.

```
1: procedure PredictCallStack(l_{target})
```

- 2: $(V, E) \leftarrow \text{GetCallGraph}()$
- 3: $f_{\text{target}} \leftarrow \text{the function containing } l_{\text{target}}$
- 4: $F_{\text{reachable}} \leftarrow \{f \mid f \in \mathbf{F} \text{ and } f \text{ can reach } f_{\text{target}} \text{ in graph } (V, E)\}$
- 5: $C_{\text{reachable}} \leftarrow \text{the concatenation of all source code in } F_{\text{reachable}}$, with the following two improvements:
 - (1) For each function, add the corresponding ===== file: function ===== at the beginning to indicate its file name and function name.
 - (2) For all call sites $l \in \{l \mid \exists (i, j, l) \in E \text{ such that } i, j \in F_{\text{reachable}}\} \cup \{l_{\text{target}}\}$, add the comment // file:line after l to indicate its file and line number.
- 6: $L_{\text{predicted}} \leftarrow \text{Call}$ the LLM interface using the prompt template in Figure 7 to obtain its output, where the parameters are <TARGET> = l_{target} , <FUNCTION> = f_{target} , <CODE> = $C_{\text{reachable}}$
- 7: **return** $L_{\text{predicted}}$

Finally, Staczzer uses the prompt template in Figure 7 to invoke the LLM (Line 6) with three parameters: the target location l_{target} , the target function f_{target} , and the code slice $C_{\text{reachable}}$. Staczzer then obtains the call stack $L_{\text{predicted}}$ predicted by the LLM and returns it (Line 7).

Figure 7 shows the prompt template used by STACZZER to invoke the LLM. This prompt template has three input parameters: the target location <TARGET>, the function containing the target location <FUNCTION>, and the source code slice <CODE>. This prompt template expects the LLM to return the backtrace call stack when a crash occurs upon triggering a vulnerability at <TARGET>. The intuition behind designing this prompt template is to repeatedly emphasize to the LLM what a correct crash call stack should look like. While being semantically correct, it should neither include extraneous stack frames that have already returned nor miss necessary call sites. We add some output examples at the end to help the LLM better understand this point.

Example 4.1. In the example shown in Section 2, assume that all three functions are located in cxxfilt.c. We have <TARGET> = cxxfilt.c:11 and <FUNCTION> = gnu_special. <CODE> is as follows:

```
1
    ==== cxxfilt.c:gnu_special =====
                                                            21
                                                                       gnu_special(mangled); // cxxfilt.c:21
    void gnu_special(const char** mangled){
                                                            22
2
                                                                     }
3
      if('0' <= **mangled && **mangled <= '9'){</pre>
                                                            23
                                                                   }else{
                                                                     if(strlen(*mangled) >= 9 && strncmp(*mangled, "
        while('0' <= **mangled && **mangled <= '9'){</pre>
                                                                           _GLOBAL_", 8) == 0 && !('0' <= (*mangled)
5
                                                                           [8] && (*mangled)[8] <= '9')){
          n *= 10:
6
7
          n += **mangled - '0';
                                                            25
                                                                       (*mangled) += 8;
                                                                       gnu_special(mangled); // cxxfilt.c:26
8
          (*mangled)++;
                                                            26
Q
                                                            27
                                                                     }
        memcpy(*output, *mangled, n); // cxxfilt.c:11
10
                                                            28
                                                                   }
11
      }
                                                            29
12
                                                            30
                                                                 }
    }
                                                            31
13
14
                                                            32
                                                                 ==== cxxfilt.c:main =====
    ==== cxxfilt.c:internal_cplus_demangle =====
16
    void internal_cplus_demangle(const char** mangled,
                                                            34
                                                                  const char** mangled = input1();
          bool flag){
                                                            35
                                                                   bool flag = input2();
17
      if(flag){
                                                            36
                                                                   internal_cplus_demangle(mangled, flag); //
18
        if(**mangled != '\0'){
                                                                         cxxfilt.c:35
          memcpy(*output, "cplus_marker", 12);
19
                                                            37
                                                                }
          (*output) += 12;
                                                            38
20
```

Prompt Template

System: You are a fuzzing expert, well-versed in the operation logic of AFL and its extension tools. You have a deep understanding of bugs inherent in the code.

Prompt Content:

You are given a codebase and a specific target line known to contain or trigger a bug, located at <TARGET> in the function <FUNCTION>. The provided code slice is <CODE>.

Output the possible call stack that would directly trigger the crash (that is, if there were a sanitizer report) based on your code understanding and static reasoning.

In the code slices, before the start of each function, ===== file:function ===== is used for indication. Each line of relevant call site is annotated with its line number in the comments. You must strictly output each call site in the file:line format.

For example, the following is a real AddressSanitizer (ASan) stack trace:

```
ERROR: AddressSanitizer: stack-buffer-
        overflow on address 0x7ffe16573d50
        at pc 0x000000549e9e bp 0
        x7ffe16572b90 sp 0x7ffe16572b88
   WRITE of size 1 at 0x7ffe16573d50 thread
2
         T0
       #0 0x549e9d in postprocess_termcap /
3
            root/ncurses/tinfo/parse_entry.
            c:1000:7
4
       #1 0x543767 in _nc_parse_entry /root
            /ncurses/tinfo/parse_entry.c
            :643:6
5
       #2 0x538e21 in _nc_read_entry_source
             /root/ncurses/tinfo/comp_parse.
            c:238:6
       #3 0x4c5c4f in main /root/progs/../
            progs/tic.c:985:5
```

In your output, only include functions that would actually appear in the final sanitizer stack trace. These must be the frames present on the stack at the moment of crash. Do not include any function that has already returned (i.e., no longer present in the stack at the time of the crash), such as

helpers or functions that were called and exited prior to the crash point.

For example, if _nc_parse_entry calls a helper function helper at parse_entry.c:700 and then helper returns, parse_entry.c:700 must not appear in this list. This is a critical selection criterion. The output should represent a single, continuous, unbroken call site chain from the innermost frame (<FUNCTION>) to the call site of the main function, as would appear in a real ASan stack trace, with no extra frames. Do not omit any function in the call stack. Please do not output any of your thinking process, only output the final result. You must strictly follow the format below: each function should be on a separate line. Do not output any additional information.

The output must not include any function that has already returned prior to the crash. Your output should strictly match what would appear in a real sanitizer stack trace, including all functions, and only those functions, that are still present on the call stack at the moment of the crash, in the correct order. Do not omit any function from the call stack. For clarity, see the following examples: [Wrong Example 1]

```
parse_entry.c:1000
    parse_entry.c:700 # <- Error: This</pre>
         function has already returned and
         MUST NOT appear here
3
    parse_entry.c:643
    comp_parse.c:238
    tic.c:985
[Wrong Example 2]
    parse_entry.c:1000 # <- Error: Missing</pre>
         the call-site in the function
         _nc_parse_entry
    comp_parse.c:238
    tic.c:985
[Correct Example]
    parse_entry.c:1000
2 parse_entry.c:643
    comp_parse.c:238
    tic.c:985
```

Fig. 7. Prompt template for guiding LLM to predict the call stack for triggering target vulnerabilities.

Algorithm 3 The algorithm to choose seed for mutation in the STACZZER framework.

Input: The set of current seeds S, and the predicted target call stack $L_{\rm predicted}$. **Output:** The seed for mutation s.

```
1: S_{\text{chosen}} \leftarrow \emptyset

2: procedure ChooseSeed(S, L_{\text{predicted}})

3: if S_{\text{chosen}} = S then

4: S_{\text{chosen}} \leftarrow \emptyset

5: S_{\text{current}} \leftarrow S - S_{\text{chosen}}

6: s \leftarrow \arg\max_{s \in S_{\text{current}}} S_{\text{corrent}}(s', L_{\text{predicted}})

7: S_{\text{chosen}} \leftarrow S_{\text{chosen}} \cup \{s\}

8: return s
```

Algorithm 4 The algorithm to assign energy for the seed for mutation in the STACZZER framework.

Input: The set of current seeds S, the seed for mutation s, and the predicted target call stack $L_{\text{predicted}}$. **Output:** The energy assigned to the seed for mutation e.

```
1: procedure AssignEnergy(S, s, L_{predicted})
2: SCORE_{average} \leftarrow \frac{\sum_{s' \in S} SCORE(s', L_{predicted})}{|S|}
3: e \leftarrow \left[ \frac{SCORE(s, L_{predicted})}{SCORE_{average}} \cdot ENERGY_{AFL}(s) \right]
4: return e
```

4.3 Seed Prioritization

Algorithm 3 formalizes the algorithm to choose seed for mutation in the Staczzer framework. This algorithm takes as input the current seed set $S \subseteq S$ and the call stack $L_{\text{predicted}} \subseteq L$ predicted by LLM. The algorithm outputs the seed $s \in S$ selected for priority mutation. Staczzer maintains a global seed set S_{chosen} representing seeds that have already been mutated (initially empty) (Line 1). If all seeds in S have been mutated (Line 3), Staczzer starts a new round by clearing S_{chosen} (Line 4). Next, Staczzer considers the seeds S_{current} that have not been mutated in the current round (Line 5). For each seed s in S_{current} , Staczzer calculates the overlap $S_{\text{core}}(s, L_{\text{predicted}})$ between its execution trace and the LLM-predicted call stack $L_{\text{predicted}}$ (Line 6), defined as follows:

$$SCORE(s, L_{predicted}) = |TRACE(s) \cap L_{predicted}|$$

STACZZER selects the seed s with the highest overlap as the seed for priority mutation, adds it to S_{chosen} (Line 7), and then returns seed s (Line 8).

Algorithm 4 formalizes the algorithm to assign energy for the seed for mutation in the STACZZER framework. The algorithm takes as input the current seed set $S \subseteq S$, the chosen seed for mutation $s \in S$, and the call stack $L_{\text{predicted}} \subseteq L$ predicted by LLM. The algorithm outputs the energy $e \in \mathbb{N}$ assigned to seed s. STACZZER calculates the average overlap SCORE_{average} between all current seed execution traces and the LLM-predicted call stack $L_{\text{predicted}}$ (Line 2). STACZZER then multiplies the original energy Energy_{AFL}(s) that AFL [32] would assign to seed s by an adjustment factor (Line 3). The factor value is the ratio between the overlap of the current seed s's execution trace with the LLM-predicted call stack $L_{\text{predicted}}$ and the average overlap. Seeds with higher overlap receive additional energy allocation. Here, Energy_{AFL}(s) is the energy heuristically assigned to each seed in AFL, based on metrics such as the seed's execution time and execution trace length. Finally, Staczzer returns the energy assigned to seed s (Line 4).

5 Experimental Evaluation

Our evaluation aims to answer the following questions:

- **RQ1.** What is the potential of the call stack-based strategy adopted by STACZZER under ideal conditions (i.e., with a completely accurate call stack)?
- **RQ2.** How effective is STACZZER at triggering targeted vulnerabilities compared to other fuzzers?
- **RQ3.** Staczzer leverages LLM to predict the target call stack based on the call graph. Can similar effectiveness be achieved using only the call graph? Is the further refinement by LLM necessary?
- **RQ4.** Can STACZZER discover new real-world vulnerabilities?

We first describe our experimental setup in Section 5.1. Then, we answer the four research questions in Section 5.2 to Section 5.5, respectively.

5.1 Experimental Setup

We conduct our experiments on Linux machines with 256 processors (2.25 GHz) and 256 GB of RAM. We implement STACZZER on top of DAFL [13] and adopt its static analysis tools. We use OpenAI o4-mini [23] as the LLM interface.

Baselines. We compare STACZZER against the following state-of-the-art fuzzers: (1) AFLGO [2], the first directed greybox fuzzer that prioritizes seeds based on the distance between seed execution traces and targets on the control flow graph. (2) WINDRANGER [7], an improvement over AFLGO that enhances distance calculation by considering only deviation basic blocks, thus effectively eliminating interference from numerous irrelevant basic blocks. (3) DAFL [13], the underlying fuzzer of our approach, which prioritizes seeds based on the distance of execution traces on the value flow graph. (4) AFL [32], which serves as the foundation for all baselines and our approach.

Benchmarks. Table 2 presents the benchmarks used in our experiments, comprising 41 known vulnerabilities from 10 programs. We show the CVE ID and vulnerability type for each vulnerability. The benchmark we use is identical to that of DAFL [13]. We compile each program with AddressSanitizer [27] instrumentation, which displays the corresponding backtrace call stack when the program crashes, enabling effective determination of whether each input can trigger the corresponding vulnerability.

Metrics. We repeat the experiments for each fuzzer on each vulnerability 40 times to eliminate the randomness introduced by random mutations in fuzzing. For each run, we set a time limit of 24 hours. Both our repetition count and time limit are identical to those used in DAFL [13]. For Staczer, we execute the LLM calls separately for each of the 40 repeated runs to eliminate the randomness in LLM inference. Our total experimental runtime is approximately 31.45 CPU-years. For each run, we place it in a dedicated Docker container and bind it to a dedicated CPU core. For each fuzzer's directed fuzzing process on each vulnerability, we record the time-to-exposure (TTE), which is the time of the first trigger of the vulnerability. We take the median of the 40 TTEs as the evaluation metric. If at least half of the 40 runs fail to trigger the vulnerability within the time limit, the median TTE cannot be calculated normally, and we uniformly set it to a penalty value of twice the time limit (48h). We consider a vulnerability to be stably reproducible by a fuzzer if and only if its median TTE can be calculated normally. Consistent with DAFL, since directed fuzzing is primarily applied to patch testing where each code change results in recompilation, the static analysis time is not a one-time cost. We include the static analysis time overhead when calculating TTE.

Table 2. Benchmarks used in the experiments. The **Type** column indicates the abbreviated type of each vulnerability: **BF** (Buffer Overflow), **NPD** (Null Pointer Dereference), **SO** (Stack Overflow), **UAF** (Use-After-Free), **IO** (Integer Overflow), **OOM** (Out-Of-Memory).

Program	Version	CVE ID	Type	Project	Program	Version	CVE ID	Type
		2016-9827	ВО		cxxfilt	2 26	2016-4490	IO
								SO
								IO
	0.4.7	2017-9988	NPD				2016-6131	SO
		2017-11728	NPD				2017-8303	BO
		2017-11729	NPD		objecty	2.28		NPD
		2017-7578	ВО		овјсору	2.20		NPD
Ming swftophp	0.4.8	2019 7869	IIAE	Binutils	-		2017-0393	NID
					objdump	2.28	2017-8392	NPD
							2017-8396	ВО
							2017-8397	ВО
							2017-8398	ВО
						0.04.4	0040 45040	
						2.31.1	2018-17360	ВО
					strip	2.27	2017-7303	NPD
					nm .	2.29	2017-14940	OOM
					readelf	2.29	2017-16828	IO
		2020-6628	ВО	-			2017 10020	
	ip 0.631	2017-8846					2017-5969	NPD
lrzip				Libxml2	xmllint	2.9.4	2017-9047	ВО
		2010-11490	UAI				2017-9048	ВО
cvvfil+	2.26	2016-4487	NPD	-		1 5 00	2018-14408	ВО
CYXIIII	2.20	2016-4489	UAF	Libjpeg	cjpeg			BO
		swftophp 0.4.8	swftophp 0.4.7 2016-9829 2016-9831 2017-9988 2017-11728 2017-11729 2017-7578 2018-7868 2018-8962 2018-11095 2018-11225 2018-11226 2018-20427 2019-9114 2019-12982 2020-6628 lrzip 0.631 2016-4487 2016-9829 2017-11728 2018-11295 2018-11296 2018-11496 2018-11496	swftophp 0.4.7 2016-9827 2016-9829 NPD 2016-9831 BO 2017-9881 NPD 2017-11728 NPD 2017-11729 NPD 2017-7578 BO 2018-7868 UAF 2018-8807 UAF 2018-8962 UAF 2018-11225 BO 2018-11226 BO 2018-20427 NPD 2019-9114 BO 2019-9114 BO 2019-12982 BO 2020-6628 BO 1rzip 0.631 2017-8846 UAF 2018-11496 UAF 2018-11496 UAF	swftophp	2016-9827 BO 2016-9829 NPD 2016-9831 BO 2017-9888 NPD 2017-11728 NPD 2017-11729 NPD 2017-7578 BO 2018-7868 UAF 2018-8807 UAF 2018-8962 UAF 2018-11095 UAF 2018-11225 BO 2018-11226 BO 2018-20427 NPD 2019-9114 BO 2019-914 BO 2019-12982 BO 2020-6628 BO 2017-8846 UAF 2018-11496 UAF 2016-4487 NPD 2016-4487 NPD	2016-9827 BO 2016-9829 NPD 2016-9831 BO Cxxfilt 2.26	Swftophp 2016-9827 BO 2016-9829 NPD 2016-9831 BO 2016-4492 2016-4492 2016-4492 2016-6131 2016-6131 2017-11728 NPD 2017-11729 NPD 2017-7578 BO 2018-8807 UAF 2018-8962 UAF 2018-11225 BO 2018-11225 BO 2018-20427 NPD 2018-20427 NPD 2019-9114 BO 2019-12982 BO 2020-6628 BO 2020-6628 BO 2020-6628 BO 2020-6628 BO 2016-4489 UAF 2016-4489

5.2 Potential of Call Stack-Based Strategy

We first conduct a controlled experiment to verify that the call stack-based strategy adopted by STACZZER has greater potential than imprecise distance metrics under optimal conditions. We denote Staczzeroptimal as the configuration where the LLM-predicted call stack is replaced with the actual call stack when triggering the target vulnerability (i.e., modifying Line 3 in Algorithm 2 to $L_{\text{predicted}} \leftarrow$ the actual call stack when triggering vulnerability at l_{target}). Table 3 shows the median TTE of this configuration and various baselines on each vulnerability. STACZZERoptimal achieves average speedups of 3.30×, 2.51×, 2.13×, and 2.16× compared to the baselines. This fully demonstrates that the call stack-based strategy can achieve dramatic improvements in DGF effectiveness after eliminating the misleading effects of imprecise static analysis information. To more intuitively show the differences between Staczzer_{optimal} and the baselines, we present the win-loss comparison between STACZZERoptimal and each baseline on every vulnerability in the Perf. vs. STACZZER_{optimal} row. For each vulnerability, we compare their median TTE values; if both cannot calculate median TTE normally, we compare which has more successful vulnerability triggers. This result is represented as a/b, where a indicates cases where STACZZER_{optimal} performs better and b indicates the opposite. The win-loss ratios of Staczzer_{optimal} compared to the baselines reach remarkable 7.5×, 4.8×, 3.38×, and 3×, further demonstrating the effectiveness of the call stackbased strategy. Based on this data, we perform a one-tailed sign test [9], where a and b represent the numbers of positive and negative signs, respectively, with results shown in the P-value in the sign test row. All p-values are far below 0.05, indicating that Staczzer_{optimal} significantly outperforms other baselines.

Table 3. Median TTE of Staczzeroptimal and each baseline over 40 runs on 41 known vulnerabilities. The **MTTE** column represents median TTE (in seconds). For cases where median TTE cannot be calculated normally, we use (x/40) to indicate, where x represents the number of runs that successfully trigger the vulnerability. The **Ratio** column shows the ratio of each fuzzer's median TTE on each vulnerability compared to Staczzeroptimal. For cases where median TTE cannot be calculated normally, it is computed using twice the time limit (48h). The best-performing fuzzer in each row is highlighted in bold. In the **Perf. vs. Staczzeroptimal** row, a/b indicates that Staczzeroptimal outperforms the fuzzer on a vulnerabilities while being outperformed on b vulnerabilities. This value is used to calculate the sign test p-value shown in the next row. The **# Stably reproducible** row indicates the number of vulnerabilities for which each fuzzer can normally calculate median TTE. The **# Best performance** row indicates the number of vulnerabilities where each fuzzer performs best.

Program	CVE ID	STACZZER _{optimal}	AFI	.Go	WINDR	ANGER	DA	FL	AFL	
8		MTTE	MTTE	Ratio	MTTE	Ratio	MTTE	Ratio	MTTE	Ratio
	2016-9827	128	461	3.60	95	0.74	147	1.15	116	0.91
	2016-9829	278	676	2.43	501	1.80	411	1.48	429	1.54
	2016-9831	183	785	4.29	459	2.51	315	1.72	416	2.27
	2017-9988	4,115	3,925	0.95	3,395	0.83	4,101	1.00	3,473	0.84
	2017-11728	530	2,815	5.31	995	1.88	631	1.19	2,364	4.46
	2017-11729	249	978	3.93	400	1.61	201	0.81	826	3.32
	2017-7578	152	845	5.56	680	4.47	643	4.23	848	5.58
	2018-7868	(0/40)	(0/40)	1.00	(0/40)	1.00	(12/40)	1.00	(0/40)	1.00
swftophp	2018-8807	(0/40)	(0/40)	1.00	(0/40)	1.00	(0/40)	1.00	(0/40)	1.00
	2018-8962	(0/40)	(0/40)	1.00	(0/40)	1.00	(2/40)	1.00	(0/40)	1.00
	2018-11095	990	8,339	8.42	2,949	2.98	2,699	2.73	6,873	6.94
	2018-11225	70,493	(8/40)	2.45	(11/40)	2.45	45,296	0.64	(13/40)	2.45
	2018-11226	58,008	(11/40)	2.98	(11/40)	2.98	62,402	1.08	(11/40)	2.98
	2018-20427	24,018	11,154	0.46	(11/40)	7.19	24,395	1.02	9,846	0.41
	2019-9114	73,775	(20/40)	2.34	(16/40)	2.34	(8/40)	2.34	(15/40)	2.34
	2019-12982	15,928	(14/40)	10.85	(13/40)	10.85	71,703	4.50	(18/40)	10.85
	2020-6628	48,511	(10/40)	3.56	(4/40)	3.56	(15/40)	3.56	(17/40)	3.56
2017-884	2017-8846	(1/40)	(1/40)	1.00	(0/40)	1.00	(1/40)	1.00	(0/40)	1.00
lrzip	2018-11496	24	193	8.04	21	0.88	25	1.04	35	1.46
	2016-4487	1,125	1,083	0.96	2,408	2.14	574	0.51	862	0.77
cxxfilt	2016-4489	500	2,628	5.26	790	1.58	2,235	4.47	1,871	3.74
	2016-4490	216	804	3.72	620	2.87	1,080	5.00	618	2.86
	2016-4491	(7/40)	(1/40)	1.00	(0/40)	1.00	(4/40)	1.00	(0/40)	1.00
	2016-4492	2,940	3,566	1.21	5,272	1.79	3,944	1.34	3,210	1.09
	2016-6131	(0/40)	(1/40)	1.00	(0/40)	1.00	(0/40)	1.00	(0/40)	1.00
	2017-8393	944	4,417	4.68	3,090	3.27	1,977	2.09	3,415	3.62
objcopy	2017-8394	878	3,563	4.06	1,268	1.44	15,029	17.12	1,367	1.56
	2017-8395	279	1,857	6.66	221	0.79	290	1.04	194	0.70
	2017-8392	321	2,209	6.88	629	1.96	361	1.12	466	1.45
	2017-8396	(0/40)	(0/40)	1.00	(1/40)	1.00	(0/40)	1.00	(1/40)	1.00
objdump	2017-8397	28,259	(17/40)	6.11	(18/40)	6.11	(7/40)	6.11	84,774	3.00
	2017-8398	3,755	6,253	1.67	2,897	0.77	4,834	1.29	5,822	1.55
	2018-17360	(0/40)	(0/40)	1.00	(0/40)	1.00	(0/40)	1.00	(4/40)	1.00
strip	2017-7303	500	3,805	7.61	5,708	11.42	667	1.33	233	0.47
nm	2017-14940	(0/40)	(0/40)	1.00	(0/40)	1.00	(0/40)	1.00	(0/40)	1.00
readelf	2017-16828	364	1,139	3.13	816	2.24	1,723	4.73	628	1.73
	2017-5969	1,117	3,166	2.83	4,647	4.16	1,410	1.26	665	0.60
xmllint	2017-9047	(18/40)	(5/40)	1.00	(2/40)	1.00	(13/40)	1.00	(5/40)	1.00
	2017-9048	52,024	(1/40)	3.32	(1/40)	3.32	13,093	0.25	(4/40)	3.32
	2018-14498	(18/40)	(2/40)	1.00	(0/40)	1.00	23,156	0.13	(11/40)	1.00
cjpeg	2020-13790	(7/40)	(1/40)	1.00	(4/40)	1.00	(6/40)	1.00	(2/40)	1.00
Aver	age ratio	-	3.3	30	2.5	51	2.1	.3	2.1	16
Perf. vs. S	FACZZE R _{optimal}	-	30	/4	29	/6	27		27	
	n the sign test	-	3 × 1	10^{-6}	5.8 ×	10^{-5}	9.4 ×	10^{-4}	2×1	10^{-3}
	reproducible	29	2	2	2		27		2:	
# Best p	erformance	21	2		5		8		6	

Table 4. Median TTE of each fuzzer over 40 runs on 41 known vulnerabilities. The **MTTE** column represents median TTE (in seconds). For cases where median TTE cannot be calculated normally, we use (x/40) to indicate, where x represents the number of runs that successfully trigger the vulnerability. The **Ratio** column shows the ratio of each fuzzer's median TTE on each vulnerability compared to STACZZER. For cases where median TTE cannot be calculated normally, it is computed using twice the time limit (48h). The best-performing fuzzer in each row is highlighted in bold. In the **Performance vs. STACZZER** row, a/b indicates that STACZZER outperforms the fuzzer on a vulnerabilities while being outperformed on b vulnerabilities. This value is used to calculate the sign test p-value shown in the next row. The **# Stably reproducible** row indicates the number of vulnerabilities for which each fuzzer can normally calculate median TTE. The **# Best performance** row indicates the number of vulnerabilities where each fuzzer performs best.

Program	CVE ID	STACZZER	AFI	.Go	WINDR	ANGER	DA	FL	AFL	
Trogram	CVLID	MTTE	MTTE	Ratio	MTTE	Ratio	MTTE	Ratio	MTTE	Ratio
	2016-9827	103	461	4.48	95	0.92	147	1.43	116	1.13
	2016-9829	227	676	2.98	501	2.21	411	1.81	429	1.89
	2016-9831	534	785	1.47	459	0.86	315	0.59	416	0.7
	2017-9988	4,402	3,925	0.89	3,395	0.77	4,101	0.93	3,473	0.7
	2017-11728	482	2,815	5.84	995	2.06	631	1.31	2,364	4.9
	2017-11729	237	978	4.13	400	1.69	287	1.21	826	3.4
	2017-7578	472	845	1.79	680	1.44	643	1.36	848	1.8
	2018-7868	(0/40)	(0/40)	1.00	(0/40)	1.00	(12/40)	1.00	(0/40)	1.0
swftophp	2018-8807	(0/40)	(0/40)	1.00	(0/40)	1.00	(0/40)	1.00	(0/40)	1.0
Swi copiip	2018-8962	(0/40)	(0/40)	1.00	(0/40)	1.00	(2/40)	1.00	(0/40)	1.0
	2018-11095	1,083	8,339	7.70	2,949	2.72	2,699	2.49	6,873	6.3
	2018-11225	38,363	(8/40)	4.50	(11/40)	4.50	45,296	1.18	(13/40)	4.5
	2018-11226	41,227	(11/40)	4.19	(11/40)	4.19	62,402	1.51	(11/40)	4.1
	2018-20427	24,635	11,154	0.45	(11/40)	7.01	24,395	0.99	9,846	0.4
	2019-9114	68,226	(20/40)	2.53	(16/40)	2.53	(8/40)	2.53	(15/40)	2.5
	2019-12982	46,618	(14/40)	3.71	(13/40)	3.71	71,703	1.54	(18/40)	3.7
	2020-6628	51,499	(10/40)	3.36	(4/40)	3.36	(15/40)	3.36	(17/40)	3.3
lrzip	2017-8846	(0/40)	(1/40)	1.00	(0/40)	1.00	(1/40)	1.00	(0/40)	1.0
11 21 p	2018-11496	20	193	9.65	21	1.05	25	1.25	35	1.7
	2016-4487	501	1,083	2.16	2,408	4.81	574	1.15	862	1.7
	2016-4489	539	2,628	4.88	790	1.47	2,235	4.15	1,871	3.4
cxxfilt	2016-4490	174	804	4.62	620	3.56	1,080	6.21	618	3.5
	2016-4491	(1/40)	(1/40)	1.00	(0/40)	1.00	(4/40)	1.00	(0/40)	1.0
	2016-4492	1,855	3,566	1.92	5,272	2.84	3,944	2.13	3,210	1.7
	2016-6131	(0/40)	(1/40)	1.00	(0/40)	1.00	(0/40)	1.00	(0/40)	1.0
	2017-8393	695	4,417	6.36	3,090	4.45	1,977	2.84	3,415	4.9
objcopy	2017-8394	1,841	3,563	1.94	1,268	0.69	15,029	8.16	1,367	0.7
	2017-8395	396	1,857	4.69	221	0.56	290	0.73	194	0.4
	2017-8392	517	2,209	4.27	629	1.22	361	0.70	466	0.9
	2017-8396	(0/40)	(0/40)	1.00	(1/40)	1.00	(0/40)	1.00	(1/40)	1.0
objdump	2017-8397	41,199	(17/40)	4.19	(18/40)	4.19	(7/40)	4.19	84,774	2.0
	2017-8398	3,560	6,253	1.76	2,897	0.81	4,834	1.36	5,822	1.6
	2018-17360	(4/40)	(0/40)	1.00	(0/40)	1.00	(0/40)	1.00	(4/40)	1.0
strip	2017-7303	499	3,805	7.63	5,708	11.44	667	1.34	233	0.4
nm	2017-14940	(0/40)	(0/40)	1.00	(0/40)	1.00	(0/40)	1.00	(0/40)	1.0
readelf	2017-16828	244	1,139	4.67	816	3.34	1,723	7.06	628	2.5
	2017-5969	1,115	3,166	2.84	4,647	4.17	1,410	1.26	665	0.6
xmllint	2017-9047	(7/40)	(5/40)	1.00	(2/40)	1.00	(13/40)	1.00	(5/40)	1.0
	2017-9048	34,856	(1/40)	4.96	(1/40)	4.96	13,093	0.38	(4/40)	4.9
-4	2018-14498	(10/40)	(2/40)	1.00	(0/40)	1.00	23,156	0.13	(11/40)	1.0
cjpeg	2020-13790	(6/40)	(1/40)	1.00	(4/40)	1.00	(6/40)	1.00	(2/40)	1.00
Ave	rage ratio	-	3.0)9	2.4	13	1.8	36	2.0)3
Performar	ice vs. Staczzer	-	31	/4	28	/7	24/	12	24/	10
P-value i	n the sign test	-	2×1	10^{-6}	2.5 ×	10^{-4}	0.0	33	0.0	12
	reproducible	29	2:		2		27		2	
	performance	20	2		5		10		6	

Additionally, Staczzer_{optimal} stably reproduces 29 vulnerabilities, the highest number among all fuzzers, further demonstrating the potential of the call stack-based strategy. Moreover, Staczzer_{optimal} achieves best performance on 21 out of 41 vulnerabilities (over 50%), showing that the call stack-based strategy makes DGF a more powerful directed vulnerability triggering tool.

Answer to RQ1: The call stack-based strategy adopted by STACZZER under ideal conditions can reproduce vulnerabilities at least 2.16× faster compared to baselines, and performs optimally in 21 out of 41 cases, fully demonstrating that this strategy has potential far exceeding conventional imprecise distance metrics.

5.3 Effectiveness

Table 4 shows the median TTE of STACZZER and various baselines. Compared to the optimal case of STACZZER optimal, STACZZER uses LLM-predicted target call stacks that, although not completely accurate, still achieve nearly comparable results. Staczzer demonstrates speedups of 3.09×, 2.43×, 1.86×, and 2.03× compared to the baselines in vulnerability reproduction, along with win-loss ratios of 7.75×, 4×, 2×, and 2.4×, fully demonstrating the effectiveness of STACZZER. The p-values from the one-tailed sign test based on win-loss counts are all below 0.05, indicating that STACZZER significantly outperforms all baselines. STACZZER can stably reproduce 29 vulnerabilities, matching STACZZER_{optimal} and outperforming all other baselines. This demonstrates from another perspective that the LLM-predicted call stack closely approximates the actual call stack. Finally, STACZZER achieves best performance on 20 out of 41 vulnerabilities, nearly half, further demonstrating that the STACZZER framework's strategy of guiding DGF through LLM-predicted target call stacks is highly efficient. Furthermore, for the vulnerability CVE-2016-4489 in program cxxfilt corresponding to the case study shown in Section 2, both Staczzeroptimal and Staczzer achieve optimal performance compared to other baselines on this vulnerability. This quantitative validation further demonstrates that the more fine-grained information used by STACZZER has more powerful effects in guiding DGF compared to conventional imprecise distance metrics.

Answer to RQ2: Staczzer can reproduce vulnerabilities at least 1.86× faster compared to baselines, and performs optimally in 20 out of 41 cases, fully demonstrating the effectiveness of Staczzer and that the LLM-predicted target call stack can closely approximate the optimization effects under optimal conditions.

5.4 Necessity of LLM Refinement

Staczzer utilizes call graph information, which differs from the control flow graphs and value flow graphs used by previous DGF approaches. To verify that the effectiveness of Staczzer stems from LLM's further refinement of coarse-grained information rather than the inherent properties of call graphs themselves, we conduct an ablation experiment. We denote Staczzerablation as the configuration that uses all target-related call sites in the call graph to guide seed prioritization (i.e., modifying Line 3 in Algorithm 2 to $L_{\text{predicted}} \leftarrow \{l \mid \exists (i, j, l) \in E \text{ such that } i, j \in F_{\text{reachable}}\} \cup \{l_{\text{target}}\}$. Table 5 shows the median TTE of Staczzerablation and Staczzer on each vulnerability. Staczzer achieves an average speedup of 1.84× and a win-loss ratio of 1.92× compared to Staczzerablation. The p-value from the one-tailed sign test based on win-loss counts is also below 0.05, indicating that Staczzer significantly outperforms Staczzerablation. Furthermore, Staczzer can stably reproduce 6 additional vulnerabilities compared to Staczzerablation, further demonstrating that Staczzer possesses stronger vulnerability triggering capabilities than Staczzerablation.

Table 5. Median TTE of each fuzzer over 40 runs on 41 known vulnerabilities in the ablation study. The **MTTE** column represents median TTE (in seconds). For cases where median TTE cannot be calculated normally, we use (x/40) to indicate, where x represents the number of runs that successfully trigger the vulnerability. The **Ratio** column shows the ratio of each fuzzer's median TTE on each vulnerability compared to STACZZER. For cases where median TTE cannot be calculated normally, it is computed using twice the time limit (48h). The best-performing fuzzer in each row is highlighted in bold. In the **Performance vs. STACZZER** row, a/b indicates that STACZZER outperforms the fuzzer on a vulnerabilities while being outperformed on b vulnerabilities. This value is used to calculate the sign test p-value shown in the next row. The # **Stably reproducible** row indicates the number of vulnerabilities for which each fuzzer can normally calculate median TTE.

Program	CVE ID	Staczzer	STACZZE	Rablation	
110511111	0,212	MTTE	MTTE	Ratio	
	2016-9827	103	93	0.90	
	2016-9829	227	330	1.45	
	2016-9831	534	416	0.78	
	2017-9988	4,402	2,626	0.60	
	2017-11728	482	1,043	2.16	
	2017-11729	237	214	0.90	
	2017-7578	472	262	0.56	
	2018-7868	(0/40)	(1/40)	1.00	
swftophp	2018-8807	(0/40)	(0/40)	1.00	
	2018-8962	(0/40)	(0/40)	1.00	
	2018-11095	1,083	3,337	3.08	
	2018-11225	38,363	(20/40)	4.50	
	2018-11226	41,227	(12/40)	4.19	
	2018-20427	24,635	(19/40)	7.01	
	2019-9114	68,226	(11/40)	2.53	
	2019-12982	46,618	(15/40)	3.71	
	2020-6628	51,499	78,994	1.53	
	2017-8846	(0/40)	(0/40)	1.00	
rzip	2018-11496	20	29	1.45	
	2016-4487	501	671	1.34	
	2016-4489	539	3,136	5.82	
xxfilt	2016-4490	174	283	1.63	
	2016-4491	(1/40)	(0/40)	1.00	
	2016-4492	1,855	2,301	1.24	

Program	CVE ID	STACZZER	STACZZER _{ablation}		
		MTTE	MTTE	Ratio	
cxxfilt	2016-6131	(0/40)	(0/40)	1.00	
	2017-8393	695	904	1.30	
objcopy	2017-8394	1,841	411	0.22	
	2017-8395	396	278	0.70	
	2017-8392	517	353	0.68	
	2017-8396	(0/40)	(0/40)	1.00	
objdump	2017-8397	41,199	65,844	1.60	
	2017-8398	3,560	5,219	1.47	
	2018-17360	(4/40)	(3/40)	1.00	
strip	2017-7303	499	634	1.27	
nm	2017-14940	(0/40)	(0/40)	1.00	
readelf	2017-16828	244	1,245	5.10	
	2017-5969	1,115	1,055	0.95	
xmllint	2017-9047	(7/40)	(6/40)	1.00	
	2017-9048	34,856	(0/40)	4.96	
	2018-14498	(10/40)	(19/40)	1.00	
cjpeg	2020-13790	(6/40)	(8/40)	1.00	
Ave	rage ratio	-	1.8	34	
Performa	nce vs. Staczzer	-	23/	12	
P-value	in the sign test	-	0.0	45	
# Stably	reproducible	29	23		

Answer to RQ3: Compared to the configuration that only uses call graph information to guide seed prioritization, Staczzer achieves an average speedup of 1.84× and optimal performance on 23 out of 41 vulnerabilities, fully demonstrating that LLM refinement of call graph information into target call stacks is necessary.

5.5 New Bugs

We use STACZZER to test the latest versions at patch locations for known fixed vulnerabilities in the projects from the controlled experiments in Table 2, with a time limit of 24 hours. We successfully discovered 10 new vulnerabilities in Binutils 2.45, as shown in Table 6. We have reported all vulnerabilities to the developers, and all vulnerabilities have been acknowledged and assigned CVE IDs. The vulnerabilities we found are located in the binary analysis tool objdump and GNU Linker 1d, both of which are widely used and highly influential tools. Among them, all vulnerabilities except CVE-2025-11839 have been confirmed and fixed by the developers. This fully demonstrates the importance of the vulnerabilities discovered by STACZZER. Furthermore, for the new vulnerabilities we discovered, we conducted additional incremental patch testing on the patched programs and

Table 6. New bugs found through regression patch testing on the latest versions of benchmarks from the controlled experiments.

Program	Location	CWE	CVE
objdump	objdump.c:4501 prdbg.c:2452	Out-of-bounds Read Unexpected Status Code or Return Value	CVE-2025-11081 CVE-2025-11839
ld	elf-eh-frame.c:756 cache.c:435 elflink.c:14898 libbfd.c:989 elflink.c:115 elf-eh-frame.c:2170 elf64-x86-64.c:4507 ldmisc.c:527	Heap-based Buffer Overflow Heap-based Buffer Overflow Out-of-bounds Read Heap-based Buffer Overflow Out-of-bounds Read Out-of-bounds Read Heap-based Buffer Overflow Out-of-bounds Read	CVE-2025-11082 CVE-2025-11083 CVE-2025-11412 CVE-2025-11413 CVE-2025-11414 CVE-2025-11494 CVE-2025-11495 CVE-2025-11840

Table 7. Incomplete fixes discovered through incremental patch testing on the patched versions of newly found vulnerabilities in Table 6.

Program	Location	CWE	Original CVE
ld	elf-eh-frame.c:766	Heap-based Buffer Overflow	CVE-2025-11082
	libbfd.c:989	Out-of-bounds Write	CVE-2025-11413

found two additional incomplete fixes, as shown in Table 7. We have submitted these to the developers and they have been successfully confirmed and further fixed. We list the CWE (Common Weakness Enumeration) for each vulnerability in both tables. These vulnerabilities existing in commonly used software may lead to very serious consequences: Heap-based Buffer Overflow and Out-of-bounds Write may cause illegal memory writes, disrupting system operation and even leading to privilege escalation; Out-of-bounds Read may cause illegal memory access, resulting in privacy information leakage. The discovery of these critical vulnerabilities greatly demonstrates the practical utility of Staczzer in real-world engineering scenarios.

Answer to RQ4: Staczzer successfully discovered 10 new vulnerabilities in high-impact software GNU Linker and related Binutils tools through regression patch testing, of which 10 have been fixed and assigned CVE IDs. Additionally, Staczzer conducted incremental patch testing on these new fixes and discovered 2 incomplete fixes that were further confirmed and patched. This fully demonstrates that Staczzer can discover critical vulnerabilities in real-world engineering scenarios and has strong practical value.

6 Discussion

We discuss potential improvements to our approach and related future research directions as follows.

Prediction of more precise metrics. We choose to have the LLM refine the call graph into a call stack as the prioritization metric. However, using call stacks to measure the likelihood that seeds mutate into target vulnerability triggers still has two limitations:

- (1) Suppose the call stack when triggering target vulnerability is $f \to g \to h$, while the critical computation statement causing the vulnerability is located in function g'. The actual call path is $f \to g \to g' \to$ (return of g') $\to h$. Since g' has already returned and is not on the call stack when the vulnerability is triggered, we cannot prioritize those critical seeds that called g'.
- (2) Call stacks can only distinguish function-level control flows. The execution paths of different seeds within functions also vary, so we cannot prioritize seeds that passed through critical basic blocks.

In fact, there are more precise alternatives that can solve these two problems, such as having the LLM refine control flow graphs/data flow graphs into precise basic block-level control flows or statement-level data flows. However, this task is still too challenging for existing LLMs. Selecting a precise path from control flow graphs or data flow graphs to trigger target vulnerabilities is unrealistic for existing LLMs. In contrast, call stacks at crash time are information more widely used in practical engineering, and LLMs have deeper understanding of such common knowledge, making call stack prediction a simpler task for LLMs. Therefore, using call stacks as the prioritization metric is actually a compromise choice where we sacrifice some guidance precision but simplify the problem into one that existing LLMs are capable of solving. Our experiments also demonstrate the effectiveness and practicality of this approach. Finally, we believe that using sufficiently precise basic block-level control flows or statement-level data flows as metrics would certainly achieve better results than using precise call stacks. Therefore, as LLM capabilities improve, using LLMs to predict more precise metrics will become a promising direction for future research.

Static analysis precision. The pointer analysis used for call graph computation is flow-insensitive and context-insensitive. More precise analysis could generate more accurate call graphs, reducing the amount of irrelevant code provided to the LLM and further enhancing LLM prediction accuracy. However, given that static analysis time is not a one-time cost in directed greybox fuzzing, more precise analysis incurs longer analysis overhead. Thus, selecting analysis with appropriate precision to achieve optimal directed vulnerability triggering efficiency involves a trade-off and constitutes a promising research direction.

Improving LLM interaction for large-scale software. We use call-graph-based code slicing and interact with LLMs through single queries, which has the advantage of negligible time overhead. However, if the software scale is too large, this approach may not be applicable because the length of code slices may exceed the token limit of LLMs. Potential improvements include:

- (1) Using agents to implement multiple interactions with LLMs, allowing the LLM to autonomously explore critical code regions and avoid feeding large amounts of useless tokens to the LLM.
- (2) Using retrieval-augmented generation (RAG) to further compress the number of input tokens by retrieving relevant code.

In fact, static analysis also consumes excessive time on large-scale software. The aforementioned methods all have the potential to eliminate static analysis and directly enable LLMs to predict precise target call stacks, which we believe is also a promising future research direction.

7 Related Work

Our approach is related to (1) directed greybox fuzzing and (2) techniques that leverage LLMs to enhance fuzzing. We summarize the related work below.

Directed greybox fuzzing. AFLGo [2] is the first directed greybox fuzzing tool that proposes using the distance from seed execution paths to targets on the control flow graph to guide seed prioritization. Building upon AFLGo, several improved methods have been proposed. CAFL [14]

additionally considers the gap between seed values and the values required to trigger vulnerabilities. WINDRANGER [7] introduces the concept of deviation basic blocks to avoid interference from irrelevant basic blocks. MC² [28] introduces Monte Carlo counting models to generate inputs that can reach targets. SelectFuzz [18] performs selective instrumentation through data dependency analysis. DAFL [13] replaces control flow graphs with value flow graphs to achieve more precise guidance. PDGF [34] obtains more precise inter-procedural control flow graphs by dynamically updating indirect calls during execution. WAFLGo [30] identifies critical code based on both control flow graphs and data flow graphs. IDFuzz [5] uses neural networks to optimize seed mutation. All these methods fail to escape imprecise distance metrics derived from static analysis. Hawkeye [3] and SDFuzz [15] leverage target call stack information to optimize directed fuzzing; however, call stack information is not easily obtainable in practical applications, and their utilization of call stacks serves only as an auxiliary role while still relying on the primarily effective imprecise distance metrics. We demonstrate in our experiments that the precise call stack adopted by STACZZER is a more effective guidance metric. Halo [12] and DeepGo [17] escape imprecise distance metrics based on invariant inference and reinforcement learning, respectively; however, they are not open-source, preventing us from comparing with them. BEACON [10] computes paths that cannot trigger targets through static analysis and terminates them early during fuzzing to improve efficiency. This is complementary to the seed prioritization improvements made by STACZZER. Additionally, there are two categories of multi-target directed greybox fuzzing techniques. Large-scale target-guided greybox fuzzing [4, 24, 35, 36] targets numerous static analysis alarms with the goal of discovering unknown vulnerabilities in programs. Critical-set directed greybox fuzzing [1, 11, 16, 26] targets a small number of known vulnerabilities with the goal of simultaneously reproducing or patchtesting multiple vulnerabilities within a single program. Both categories of techniques are based on conventional distance metrics; therefore, the precise call stack metrics introduced by Staczzer can be well integrated with these methods to further enhance effectiveness.

Fuzzing with LLMs. With the powerful code understanding and generation capabilities, LLMs have been widely applied to generate initial corpora and mutators for fuzzing programs with structured inputs, including compilers [29, 31], interpreters [8, 29, 31], theorem provers [29], non-textual inputs (such as videos, images, PDFs, etc.) [33], deep learning libraries [6], protocol specifications [20], and others. LLMs have also been used to automatically generate harnesses for library functions [19]. Finally, LLMs have been employed in directed fuzzing to generate initial corpora that are more likely to trigger vulnerabilities [37]. STACZZER is the first work to introduce LLMs into the core seed prioritization component of directed greybox fuzzing. Moreover, STACZZER is orthogonal to the aforementioned works and can be combined with them to achieve better results.

8 Conclusion

We present Staczer, a framework that leverages LLMs to predict call stacks when triggering target vulnerabilities to guide seed prioritization in directed greybox fuzzing. Staczer evaluates the overlap between each seed's execution path and the predicted call stack, considering seeds with higher overlap more likely to mutate into target vulnerability triggers and prioritizing their mutation. We conducted experiments totaling over 31.45 CPU-years to validate the effectiveness of Staczer. Staczer reproduces known vulnerabilities with average speedups of 1.86× to 3.09× compared to baselines, while discovering 10 new vulnerabilities and 2 incomplete fixes, with 10 assigned CVE IDs. These results fully demonstrate that Staczer achieves powerful directed vulnerability triggering capabilities compared to existing directed fuzzers.

References

- [1] Andrew Bao, Wenjia Zhao, Yanhao Wang, Yueqiang Cheng, Stephen McCamant, and Pen-Chung Yew. 2025. From Alarms to Real Bugs: Multi-target Multi-step Directed Greybox Fuzzing for Static Analysis Result Verification. In 34th USENIX Security Symposium (USENIX Security 25). 6977–6997. https://www.usenix.org/system/files/usenixsecurity25-bao-andrew.pdf
- [2] Marcel Böhme, Van-Thuan Pham, Manh-Dung Nguyen, and Abhik Roychoudhury. 2017. Directed Greybox Fuzzing. In Proceedings of the 2017 ACM SIGSAC Conference on Computer and Communications Security, CCS 2017, Dallas, TX, USA, October 30 - November 03, 2017, Bhavani Thuraisingham, David Evans, Tal Malkin, and Dongyan Xu (Eds.). ACM, 2329–2344. doi:10.1145/3133956.3134020
- [3] Hongxu Chen, Yinxing Xue, Yuekang Li, Bihuan Chen, Xiaofei Xie, Xiuheng Wu, and Yang Liu. 2018. Hawkeye: Towards a Desired Directed Grey-box Fuzzer. In Proceedings of the 2018 ACM SIGSAC Conference on Computer and Communications Security, CCS 2018, Toronto, ON, Canada, October 15-19, 2018, David Lie, Mohammad Mannan, Michael Backes, and XiaoFeng Wang (Eds.). ACM, 2095–2108. doi:10.1145/3243734.3243849
- [4] Yaohui Chen, Peng Li, Jun Xu, Shengjian Guo, Rundong Zhou, Yulong Zhang, Tao Wei, and Long Lu. 2020. SAVIOR: Towards Bug-Driven Hybrid Testing. In 2020 IEEE Symposium on Security and Privacy, SP 2020, San Francisco, CA, USA, May 18-21, 2020. IEEE, 1580–1596. doi:10.1109/SP40000.2020.00002
- [5] Yiyang Chen, Chao Zhang, Long Wang, Wenyu Zhu, Changhua Luo, Nuoqi Gui, Zheyu Ma, Xingjian Zhang, and Bingkai Su. 2025. {IDFuzz}: Intelligent Directed Grey-box Fuzzing. In 34th USENIX Security Symposium (USENIX Security 25). 6219–6238. https://www.usenix.org/system/files/usenixsecurity25-chen-yiyang.pdf
- [6] Yinlin Deng, Chunqiu Steven Xia, Haoran Peng, Chenyuan Yang, and Lingming Zhang. 2023. Large Language Models Are Zero-Shot Fuzzers: Fuzzing Deep-Learning Libraries via Large Language Models. In Proceedings of the 32nd ACM SIGSOFT International Symposium on Software Testing and Analysis, ISSTA 2023, Seattle, WA, USA, July 17-21, 2023, René Just and Gordon Fraser (Eds.). ACM, 423-435. doi:10.1145/3597926.3598067
- [7] Zhengjie Du, Yuekang Li, Yang Liu, and Bing Mao. 2022. Windranger: A Directed Greybox Fuzzer driven by Deviation Basic Blocks. In 44th IEEE/ACM 44th International Conference on Software Engineering, ICSE 2022, Pittsburgh, PA, USA, May 25-27, 2022. ACM, 2440–2451. doi:10.1145/3510003.3510197
- [8] Jueon Eom, Seyeon Jeong, and Taekyoung Kwon. 2024. Fuzzing JavaScript Interpreters with Coverage-Guided Reinforcement Learning for LLM-Based Mutation. In Proceedings of the 33rd ACM SIGSOFT International Symposium on Software Testing and Analysis, ISSTA 2024, Vienna, Austria, September 16-20, 2024, Maria Christakis and Michael Pradel (Eds.). ACM, 1656–1668. doi:10.1145/3650212.3680389
- [9] Myles Hollander, Douglas A Wolfe, and Eric Chicken. 2013. Nonparametric statistical methods. John Wiley & Sons.
- [10] Heqing Huang, Yiyuan Guo, Qingkai Shi, Peisen Yao, Rongxin Wu, and Charles Zhang. 2022. BEACON: Directed Grey-Box Fuzzing with Provable Path Pruning. In 43rd IEEE Symposium on Security and Privacy, SP 2022, San Francisco, CA, USA, May 22-26, 2022. IEEE, 36-50. doi:10.1109/SP46214.2022.9833751
- [11] Heqing Huang, Peisen Yao, Hung-Chun Chiu, Yiyuan Guo, and Charles Zhang. 2024. Titan: Efficient Multi-target Directed Greybox Fuzzing. In IEEE Symposium on Security and Privacy, SP 2024, San Francisco, CA, USA, May 19-23, 2024. IEEE, 1849–1864. doi:10.1109/SP54263.2024.00059
- [12] Heqing Huang, Anshunkang Zhou, Mathias Payer, and Charles Zhang. 2024. Everything is Good for Something: Counterexample-Guided Directed Fuzzing via Likely Invariant Inference. In IEEE Symposium on Security and Privacy, SP 2024, San Francisco, CA, USA, May 19-23, 2024. IEEE, 1956–1973. doi:10.1109/SP54263.2024.00142
- [13] Tae Eun Kim, Jaeseung Choi, Kihong Heo, and Sang Kil Cha. 2023. DAFL: Directed Grey-box Fuzzing guided by Data Dependency. In 32nd USENIX Security Symposium, USENIX Security 2023, Anaheim, CA, USA, August 9-11, 2023, Joseph A. Calandrino and Carmela Troncoso (Eds.). USENIX Association, 4931–4948. https://www.usenix.org/conference/usenixsecurity23/presentation/kim-tae-eun
- [14] Gwangmu Lee, Woochul Shim, and Byoungyoung Lee. 2021. Constraint-guided Directed Greybox Fuzzing. In 30th USENIX Security Symposium, USENIX Security 2021, August 11-13, 2021, Michael D. Bailey and Rachel Greenstadt (Eds.). USENIX Association, 3559–3576. https://www.usenix.org/conference/usenixsecurity21/presentation/lee-gwangmu
- [15] Penghui Li, Wei Meng, and Chao Zhang. 2024. SDFuzz: Target States Driven Directed Fuzzing. In 33rd USENIX Security Symposium, USENIX Security 2024, Philadelphia, PA, USA, August 14-16, 2024, Davide Balzarotti and Wenyuan Xu (Eds.). USENIX Association. https://www.usenix.org/conference/usenixsecurity24/presentation/li-penghui
- [16] Hongliang Liang, Xinglin Yu, Xianglin Cheng, Jie Liu, and Jin Li. 2024. Multiple Targets Directed Greybox Fuzzing. IEEE Trans. Dependable Secur. Comput. 21, 1 (2024), 325–339. doi:10.1109/TDSC.2023.3253120
- [17] Peihong Lin, Pengfei Wang, Xu Zhou, Wei Xie, Gen Zhang, and Kai Lu. 2024. DeepGo: Predictive Directed Greybox Fuzzing. In 31st Annual Network and Distributed System Security Symposium, NDSS 2024, San Diego, California, USA, February 26 - March 1, 2024. The Internet Society. https://www.ndss-symposium.org/ndss-paper/deepgo-predictive-directed-greybox-fuzzing/

- [18] Changhua Luo, Wei Meng, and Penghui Li. 2023. SelectFuzz: Efficient Directed Fuzzing with Selective Path Exploration. In 44th IEEE Symposium on Security and Privacy, SP 2023, San Francisco, CA, USA, May 21-25, 2023. IEEE, 2693–2707. doi:10.1109/SP46215.2023.10179296
- [19] Yunlong Lyu, Yuxuan Xie, Peng Chen, and Hao Chen. 2024. Prompt Fuzzing for Fuzz Driver Generation. In Proceedings of the 2024 on ACM SIGSAC Conference on Computer and Communications Security, CCS 2024, Salt Lake City, UT, USA, October 14-18, 2024, Bo Luo, Xiaojing Liao, Jun Xu, Engin Kirda, and David Lie (Eds.). ACM, 3793–3807. doi:10.1145/ 3658644.3670396
- [20] Ruijie Meng, Martin Mirchev, Marcel Böhme, and Abhik Roychoudhury. 2024. Large Language Model guided Protocol Fuzzing. In 31st Annual Network and Distributed System Security Symposium, NDSS 2024, San Diego, California, USA, February 26 - March 1, 2024. The Internet Society. https://www.ndss-symposium.org/ndss-paper/large-language-model-guided-protocol-fuzzing/
- [21] MITRE. 2016. CVE-2016-4489. https://cve.mitre.org/cgi-bin/cvename.cgi?name=CVE-2016-4489.
- [22] MITRE. 2017. CVE-2017-8398. https://cve.mitre.org/cgi-bin/cvename.cgi?name=CVE-2017-8398.
- [23] OpenAI. 2025. o4-mini. https://platform.openai.com/docs/models/o4-mini.
- [24] Sebastian Österlund, Kaveh Razavi, Herbert Bos, and Cristiano Giuffrida. 2020. ParmeSan: Sanitizer-guided Greybox Fuzzing. In 29th USENIX Security Symposium, USENIX Security 2020, August 12-14, 2020, Srdjan Capkun and Franziska Roesner (Eds.). USENIX Association, 2289–2306. https://www.usenix.org/conference/usenixsecurity20/presentation/osterlund
- [25] Henry Gordon Rice. 1953. Classes of recursively enumerable sets and their decision problems. *Transactions of the American Mathematical society* 74, 2 (1953), 358–366.
- [26] Huanyao Rong, Wei You, Xiaofeng Wang, and Tianhao Mao. 2024. Toward Unbiased Multiple-Target Fuzzing with Path Diversity. In 33rd USENIX Security Symposium, USENIX Security 2024, Philadelphia, PA, USA, August 14-16, 2024, Davide Balzarotti and Wenyuan Xu (Eds.). USENIX Association. https://www.usenix.org/conference/usenixsecurity24/ presentation/rong
- [27] Konstantin Serebryany, Derek Bruening, Alexander Potapenko, and Dmitriy Vyukov. 2012. AddressSanitizer: A Fast Address Sanity Checker. In *Proceedings of the 2012 USENIX Annual Technical Conference, USENIX ATC 2012, Boston, MA, USA, June 13-15, 2012*, Gernot Heiser and Wilson C. Hsieh (Eds.). USENIX Association, 309–318. https://www.usenix.org/conference/atc12/technical-sessions/presentation/serebryany
- [28] Abhishek Shah, Dongdong She, Samanway Sadhu, Krish Singal, Peter Coffman, and Suman Jana. 2022. MC2: Rigorous and Efficient Directed Greybox Fuzzing. In Proceedings of the 2022 ACM SIGSAC Conference on Computer and Communications Security, CCS 2022, Los Angeles, CA, USA, November 7-11, 2022, Heng Yin, Angelos Stavrou, Cas Cremers, and Elaine Shi (Eds.). ACM, 2595–2609. doi:10.1145/3548606.3560648
- [29] Chunqiu Steven Xia, Matteo Paltenghi, Jia Le Tian, Michael Pradel, and Lingming Zhang. 2024. Fuzz4All: Universal Fuzzing with Large Language Models. In Proceedings of the 46th IEEE/ACM International Conference on Software Engineering, ICSE 2024, Lisbon, Portugal, April 14-20, 2024. ACM, 126:1–126:13. doi:10.1145/3597503.3639121
- [30] Yi Xiang, Xuhong Zhang, Peiyu Liu, Shouling Ji, Xiao Xiao, Hong Liang, Jiacheng Xu, and Wenhai Wang. 2024. Critical Code Guided Directed Greybox Fuzzing for Commits. In 33rd USENIX Security Symposium, USENIX Security 2024, Philadelphia, PA, USA, August 14-16, 2024, Davide Balzarotti and Wenyuan Xu (Eds.). USENIX Association. https://www.usenix.org/conference/usenixsecurity24/presentation/xiang-yi
- [31] Yupeng Yang, Shenglong Yao, Jizhou Chen, and Wenke Lee. 2025. Hybrid Language Processor Fuzzing via {LLM-Based} Constraint Solving. In 34th USENIX Security Symposium (USENIX Security 25). 6299–6318. https://www.usenix.org/system/files/usenixsecurity25-yang-yupeng.pdf
- [32] Michał Zalewski. 2013. American Fuzzy Lop. https://lcamtuf.coredump.cx/afl/.
- [33] Kunpeng Zhang, Zongjie Li, Daoyuan Wu, Shuai Wang, and Xin Xia. 2025. Low-Cost and Comprehensive Non-textual Input Fuzzing with LLM-Synthesized Input Generators. arXiv preprint arXiv:2501.19282 (2025). https://www.usenix.org/system/files/conference/usenixsecurity25/sec25cycle1-prepub-1291-zhang-kunpeng.pdf
- [34] Yujian Zhang, Yaokun Liu, Jinyu Xu, and Yanhao Wang. 2024. Predecessor-aware Directed Greybox Fuzzing. In IEEE Symposium on Security and Privacy, SP 2024, San Francisco, CA, USA, May 19-23, 2024. IEEE, 1884–1900. doi:10.1109/ SP54263.2024.00040
- [35] Zhijie Zhang, Liwei Chen, Haolai Wei, Gang Shi, and Dan Meng. 2024. Prospector: Boosting Directed Greybox Fuzzing for Large-Scale Target Sets with Iterative Prioritization. In Proceedings of the 33rd ACM SIGSOFT International Symposium on Software Testing and Analysis, ISSTA 2024, Vienna, Austria, September 16-20, 2024, Maria Christakis and Michael Pradel (Eds.). ACM, 1351–1363. doi:10.1145/3650212.3680365
- [36] Han Zheng, Jiayuan Zhang, Yuhang Huang, Zezhong Ren, He Wang, Chunjie Cao, Yuqing Zhang, Flavio Toffalini, and Mathias Payer. 2023. FISHFUZZ: Catch Deeper Bugs by Throwing Larger Nets. In 32nd USENIX Security Symposium, USENIX Security 2023, Anaheim, CA, USA, August 9-11, 2023, Joseph A. Calandrino and Carmela Troncoso (Eds.). USENIX Association, 1343–1360. https://www.usenix.org/conference/usenixsecurity23/presentation/zheng

[37] Zhuotong Zhou, Yongzhuo Yang, Susheng Wu, Yiheng Huang, Bihuan Chen, and Xin Peng. 2024. Magneto: A Step-Wise Approach to Exploit Vulnerabilities in Dependent Libraries via LLM-Empowered Directed Fuzzing. In Proceedings of the 39th IEEE/ACM International Conference on Automated Software Engineering, ASE 2024, Sacramento, CA, USA, October 27 - November 1, 2024, Vladimir Filkov, Baishakhi Ray, and Minghui Zhou (Eds.). ACM, 1633–1644. doi:10.1145/3691620.3695531